RSC Advances

PAPER

View Article Online
View Journal | View Issue



Cite this: *RSC Adv.*, 2018, **8**, 32490

# Crystal structures, and magnetic and thermal properties of basic copper formates with two-dimensional triangular-lattice magnetic networks†

Wataru Fujita *

Received 27th August 2018
Accepted 13th September 2018

DOI: 10.1039/c8ra07134a

rsc.li/rsc-advances

Basic copper formate, $[Cu_3(OH)_4(HCOO)_2]$, was selectively prepared by hydrolysis of formate ions in concentrated aqueous solutions of copper formate. This material exhibits a two-dimensional distorted triangular-lattice magnetic network of Cu(II) ions where $S = 1/2$. The dominance of antiferromagnetic interactions with $J/k_B = 35.7(2)$ K and a magnetic anomaly at approximately 2.3 K that corresponds to a paramagnetic-to-antiferromagnetic ordering transition were revealed by magnetic measurements. The field dependence of the magnetisation at 2 K corresponds to the 1/3-magnetisation plateau that is commonly observed in a two-dimensional triangular-lattice system. Moreover, heat-capacity measurements found a λ-type anomaly at 2.15 K, which is the magnetic transition temperature. This material may be a good candidate for a geometrical frustration system with novel magnetic phenomena such as spin-liquid states.



## Introduction

Copper hydroxide salts $(Cu(OH)_{2-x}A_{x/n}\cdot mH_2O$, in which A is an $n$th-valent anion) are of particular interest in the field of magnetism. More specifically, a number of these salts exhibit $S = 1/2$ frustrated magnetic networks, such as two-dimensional triangular lattices, kagomé lattices, pyrochlore-like lattices, and diamond-chain lattices, among others.[1,2] In such magnetic networks, novel magnetic phenomena such as spin-liquid states, spin-glass-like behaviour, and idle spin states have been observed.[3–5]

The crystal structures and magnetic properties of copper hydroxide salts are known to depend on factors such as the molecular structure and valency of the anion $A^{n-}$, or the proportions of $Cu^{2+}$, $OH^-$, $A^{n-}$, and $H_2O$.[6] To explore copper hydroxide derivatives that exhibit potentially attractive properties, it is necessary to carry out preparative, detailed structural, and magnetic investigations into such derivatives. For example, a range of anions, and in particular organic anions, that exhibit structural variety could be examined. Although single crystals of layered metal hydroxides containing inorganic guest ions can be prepared by hydrothermal methods,[7] organic derivatives decompose at high temperatures, and so are rarely obtained *via* such methods.[8] Indeed, the preparation and structural analyses of the formate $[Cu_2(OH)_3(HCOO)]$,[9] acetate $[Cu_2(OH)_3(CH_3COO)]\cdot H_2O$,[10] and propionate $[Cu_7(OH)_{12}(CH_3CH_2CO_2)_2]\cdot(CH_3CH_2CO_2H)_2\cdot(H_2O)_6$ (ref. 11) derivatives have been reported through the hydrolyses of their corresponding carboxylate ions at low temperatures. Furthermore, copper hydroxides bearing organic sulfonate ions $(RSO_3^-)$ were successfully prepared by the hydrolysis of acetate ions, and these compounds were shown to exhibit two-dimensional triangular-lattice or diamond-chain-lattice magnetic networks.[12] In addition, Evrard *et al.* recently reported the successful preparation of single crystals of copper hydroxides with the decanesulfate anion $(A = n\text{-}C_{12}H_{25}SO_4^-)$ by hydrolysis, and discussed their magnetic properties, among others.[13] The hydrolysis methods are useful for preparation of single crystals of metal hydroxides with various anions and will contribute structural chemistry of them.

It is known that there are three kinds of basic copper formates $(A = HCOO^-)$, $[Cu_3(OH)_4(HCOO)_2]$ (**1**),[14] $[Cu_2(OH)_3(HCOO)]$ (**2**),[9] and $[Cu(OH)(HCOO)]$ (**3**).[14] More specifically, compounds **2** and **3** have crystallographically determined layered structures; in particular, **2** has a two-dimensional triangular-lattice magnetic network with dominant ferromagnetic interactions.[9] In the case of compound **1**, the positions of the copper atoms in its crystal structure have been determined by Weissenberg photography,[14] and the atomic alignment of its copper atoms was found to be triangular-lattice-like. However, detailed structural analyses have not yet been reported for these compounds. It is also noted that compound **1** has an associated Weiss constant of −17.3 K, indicating that dominant antiferromagnetic interactions exist between its copper ions.

*General Education, Faculty of Science and Technology, Seikei University, 3-3-1 Kichijoji-kitamachi, Musashino-shi, Tokyo 180-8633, Japan. E-mail: fujitaw@st.seikei.ac.jp; Fax: +81-422-37-3781; Tel: +81-422-37-3792*

† Electronic supplementary information (ESI) available: Photograph of by products, infrared spectrum of **1**, crystal structure of **2** and **3**, magnetic interaction pathways in **1**. CCDC 1851893 and 1859854. For ESI and crystallographic data in CIF or other electronic format see DOI: 10.1039/c8ra07134a

Compound **1** also has a magnetic anomaly at approximately 2.5 K.[14] As geometrical frustration can occur in a triangular lattice with working antiferromagnetic couplings, compound **1** can be considered a good candidate for a spin-frustrated system.

Thus, the author herein reports our investigation of the crystal growth by hydrolysis methods, structure, and magnetic and thermal properties of the pure phase of the basic copper formate **1**. The structural and magnetic differences between **1** and **2** are also described in detail, and the crystal structure of **3** is re-analysed.

# Experimental

### Preparation of 1

A solution of copper formate tetrahydrate (20 g) in water (200 mL) was heated at 70 °C for 3 hours. The resulting greenish powder was removed by filtration, and the filtrate was heated at 70 °C in a water bath for one days. After this time, the resulting microcrystalline powder was removed by filtration, and the filtrate was maintained at 70 °C for 6 d to yield dark green plate-like crystals, which were collected by filtration. Yield of the plate crystals: 1.38 g. Anal. calcd for $C_2H_6O_8Cu_3$: C, 6.89%; H, 1.73%; found: C, 6.88%; H, 1.74%. Characteristic IR bands ($cm^{-1}$): 3296 (shoulder), 3211 (s), 2859 (m), 2740 (w), 2639 (vw), 2072 (m), 1555 (vs), 1378 (vs), 1333 (vs), 1954 (m), 921 (m), 889 (m), 829 (vs), 745 (vs), 517 (m), 486 (s), 454 (s).

### Preparation of 3

Compound **3** was prepared according to a previously reported literature procedure.[14]

### IR spectrum of 1

Fourier transform infrared (FT-IR) spectroscopic analysis was performed on a Shimadzu IRSpirit spectrometer with a diamond ATR option.

### Structural analyses of 1 and 3

X-ray diffraction data were collected on a Rigaku Mercury CCD diffractometer, using graphite-monochromated Mo-K$\alpha$ ($\lambda$ = 0.71073 Å) radiation. All structures were solved by means of the SHELXT program using the dual-space method and refining by successive differential Fourier syntheses and a full-matrix least-squares procedure.[15,16] Anisotropic thermal factors were applied to all non-hydrogen atoms. The crystal parameters obtained for compounds **1–3** are summarised in Table 1. Crystallographic data have been deposited at the Cambridge Crystallographic Data Centre (CCDC-1851893 and 1859854 for compounds **1** and **3**, respectively).

### Magnetic measurements involving 1

Microcrystalline samples in gelatin capsules were subjected to SQUID magnetometer (Quantum Design MPMS XL-7). DC magnetic measurements were carried out at 500 Oe and 2–300 K. The field dependence of the magnetisation was measured at both 2 and 20 K. The molar units of $\chi_p$ and magnetisation were represented as the quantity per mole of Cu. The experimentally obtained raw data were corrected for the diamagnetism[17] of the sample and the gelatin capsule, and the molar paramagnetic susceptibilities were obtained.

### Heat capacities of 1

Heat capacities of **1** were measured for the plate-like crystals (1.473 mg) at the Coordinated Center for UEC Research Facilities, The University of Electro-communications, using a Quantum Design PPMS instrument equipped with a relaxation-type calorimeter option. The molar units of $C_p$ were represented as the quantity per mole of Cu. The magnetic heat capacity $C_{mag}$ was obtained by subtracting the lattice contribution $C_{lattice}$ from the total heat capacity $C_p$. The lattice heat capacity $C_{lattice}$ was determined by fitting the $C_p$ data over the 2–30 K temperature range to a polynomial. The magnetic entropy was obtained by integrating $C_{mag}/T$ over the 2.2–30 K range.

# Results and discussion

### Preparation

Preparation of the basic copper formate compounds **1–3** was previously reported in the literature.[9,14,18,19] More specifically, as part of a study into the decomposition of metal formates, Riban prepared **1** by boiling saturated solutions of copper formate.[18] In addition, Fowles prepared **2** by boiling dilute solutions of copper formate,[19] while Euler *et al.* determined the crystal structure of **2**[9] using the single crystals prepared by the method of Fowles. Similarly, Mori *et al.* reported a detailed preparative method for **3**, in addition to examination of the crystal structure and magnetic properties of this compound.[14] However, detailed conditions for the preparation of **1** and **2** were not reported. Previously, the author explored the reaction conditions for the preparation of single-crystalline **2**,[9] which was obtained by heating an aqueous solution (100 mL) of copper formate tetrahydrate (2 g) at 75–80 °C. In general, formate ions reduce copper ions at high temperatures. Indeed, significant quantities of dark reddish crystals of the reduction product, $Cu_2O$, were formed at

Table 1 Crystallographic data for **1–3**

| | **1** | **2** | **3** |
|---|---|---|---|
| Formula | $[Cu_3(OH)_4(HCOO)_2]$ | $[Cu_2(OH)_3(HCOO)]$ | $[Cu(OH)(HCOO)]$ |
| Crystal system | Monoclinic | Monoclinic | Monoclinic |
| Space group | $P2_1/c$ | $P2_1$ | $P2_1/m$ |
| $a$/Å | 7.0572(7) | 5.592(12) | 3.2574(12) |
| $b$/Å | 9.1203(7) | 6.065(12) | 5.9387(14) |
| $c$/Å | 5.7992(5) | 6.919(14) | 7.246(3) |
| $\beta$/° | 105.878(4) | 105.94(2) | 101.805(9) |
| $V$/Å$^3$ | 359.02(6) | 225.6(8) | 137.21(8) |
| $Z$ | 2 | 2 | 2 |
| $R_1$ | 0.0398 | 0.0631 | 0.0296 |
| w$R_2$ | 0.0974 | 0.1773 | 0.0755 |
| $T$/K | 290 | 273(2) | 130(2) |
| Ref. | This work | 9 | This work |

reaction temperatures >75 °C (Fig. S1†). It therefore appeared that boiling was unfavourable for the preparation of the pure phase.

The author subsequently explored the preparation of basic copper formate using copper formate solutions of varying concentrations and using temperatures lower than those reported in the preceding work. More specifically, aqueous solutions (100 mL) containing copper formate tetrahydrate (2, 5, and 10 g) were heated at temperatures ≤70 °C to give a greenish powder. As this powder inhibits single-crystal growth, it was removed by filtration in all cases, and each filtrate was re-heated to the desired temperature once again. Distilled water was then added when amount of the solution decreased by evaporation of water. Where <5 g copper formate tetrahydrate was employed, the main isolated product was **2**, although small quantities of **1** were also obtained. However, upon heating over a prolonged period of time, **1** was formed as the main product, and only **1** was formed when 10 g copper formate tetrahydrate was employed. Under these conditions, only trace quantities of $Cu_2O$ were detected in the product. Although compound **1** was formed at temperatures <70 °C (*e.g.*, at 40 °C), the rate of crystal growth was slower than at 70 °C. Single crystals measuring 2.0 × 1.0 × 0.03 mm were grown over several weeks, and a photographic image of these crystals is shown in Fig. 1. It was therefore apparent that the crystal growth conditions employed in this study affected the products formed from the copper hydroxide derivatives, and the conditions for the formation for **1** were elucidated herein.

## Crystal structure

The structures of the obtained crystals were determined by X-ray crystallography. The crystallographic data pertaining to compounds **1–3** are summarised in Table 1; the crystal structures of **2** and **3** were previously reported, the structures of which are shown in Fig. S3 and S4.† However, the preparation and structure of **3** were re-examined in this study. More specifically, the structure of **3** was previously reported to belong to the $P2_1$ space group;[14] however, the results in this study indicated that it belongs to the $P2_1/m$ space group. In addition, it is noted that compound **2** consists of a two-dimensional triangular-lattice alignment of copper ions (Fig. S3†), while **3** consists of a square-planar lattice with diagonal magnetic paths (Fig. S4†).

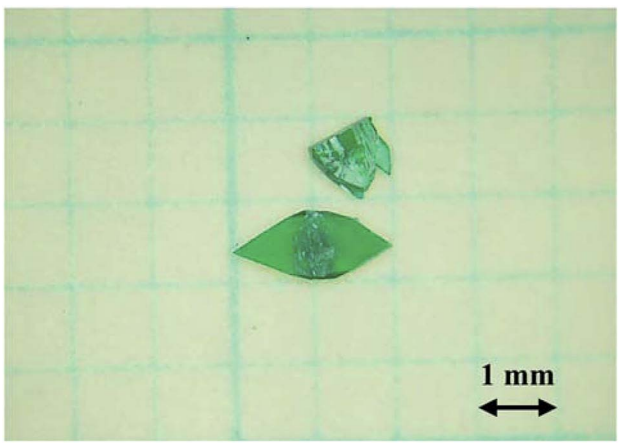


Fig. 1 Photograph of single crystals of **1**.

Thus, as determined herein, compound **1** contains three copper ions, four hydroxide ions, and two formate ions, which confirms the results reported by Mori *et al.*[14] The crystal structure of **1** is shown in Fig. 2, where it is apparent that **1** crystallised in the centrosymmetric $P2_1/c$ space group with half of its formula unit being crystallographically asymmetric. In addition, compound **1** also consists of a layered structure with sheets in the *bc* plane that are stacked along the *a* axis (see Fig. 2(a)). These layers are well separated by the formyl groups of the formate ions present in the interlayers. In addition, Fig. 2(b) shows the projection of the above-mentioned layer toward the *a* axis. Interestingly, the atomic alignment of the layer in **1** is similar to that observed for brucite $Mg(OH)_2$,[20] in that the magnesium ions are substituted by copper ions and the $OH^-$ ions are partially substituted by formate ions. It is also noted that the structural features of **1** are similar to those of **2** (Fig. S3†). The layers present in **2** consist of edge-sharing $CuO_6$ octahedra, where each copper atom is bridged by two oxygen atoms to form a two-dimensional triangular-lattice magnetic network within the layer. It is also possible that neighbouring copper ions interact magnetically *via* the oxygen atoms. Furthermore, two types of Cu–O bonds exist in the $CuO_6$ octahedra, which is a consequence of Jahn–Teller distortion, thereby rendering all copper ions divalent with a spin of 1/2. The lengths of the axial and equatorial bonds in **2** are 2.256(4)–2.715(4) and 1.919(3)–2.061(3)° Å, respectively. Moreover, the triangular alignments of the copper ions are not structurally regular since the Cu–O–Cu bridges have bond angles of 84.49(11)–106.63(14)° that are chemically inequivalent. The superexchange interactions in the copper hydroxide compounds that occur through Cu–O–Cu bridges are sensitive to these angles[21] and so on.[22] As indicated in Fig. S5,† five kinds of magnetic-interaction pathways exist, which are associated with the magnetic coupling constants $J_1$–$J_5$.

Fig. 2(c) shows a schematic representation of the layers present in **1**, where the axial Cu–O bonds and the oxygen atoms of the formate ions coordinated to the copper ions are highlighted. In addition, the axial and equatorial Cu–O bonds in the elongated $CuO_6$ octahedra are represented by bold and narrow black lines, respectively. Although the atomic alignment of **1** is similar to that of **2**, the coordination positions and numbers of the formate ions in **1** differ to those in **2** (Fig. S3(c)†). The oxygen atoms of the formate ions coordinated to the copper ions are represented by bold red and magenta atomic symbols, thereby indicating that the oxygen atoms are located at the front and rear of the copper hydroxide layer, respectively. Furthermore, the formate ions in **1** are coordinated to three copper ions and two of these coordination bonds are axial with respect to the copper ions, while the formate ions form three axial bonds with the copper ions in **2**. Moreover, the anionic species are also axially coordinated to the copper ions, as previously reported in the case of basic copper salts.[9,11,12] As the $CuO_6$ octahedra in **1** are oriented differently to those in **2**, it is expected that

 

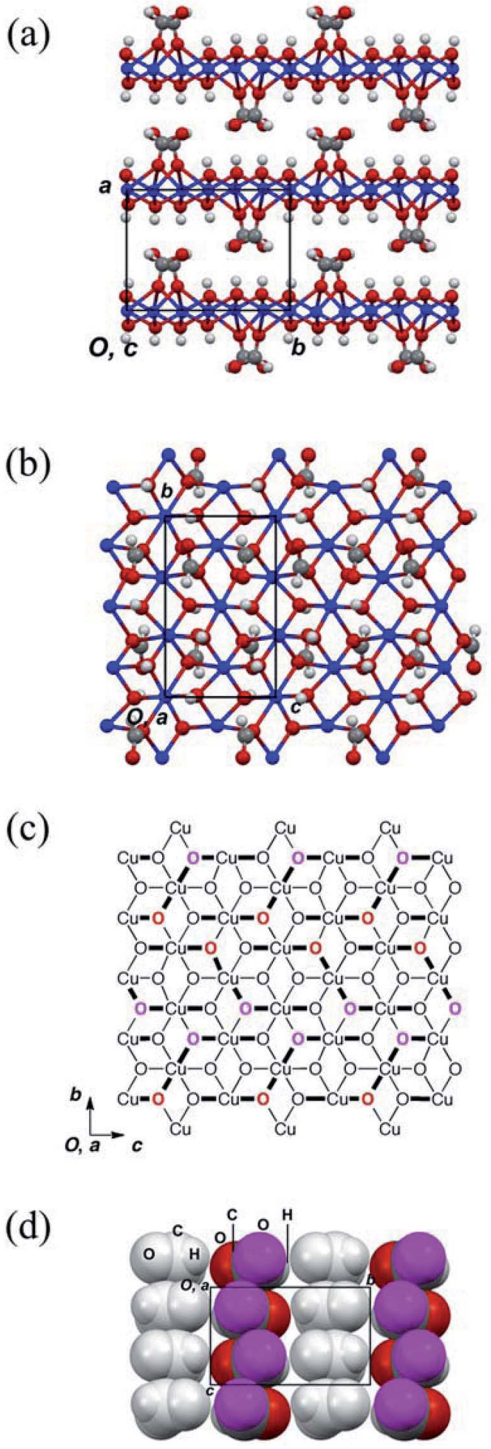


Fig. 2 Crystal structure of **1**. Spheres correspond to Cu (blue, green), O (red or magenta), C (dark grey), and H (light grey). (a) Stacking of the copper hydroxide layers. (b) Projection of the arrangement of the copper hydroxide layer along the *a* axis. (c) Schematic representation of the copper hydroxide layer of **1**. The bold lines are the axial bonds. Coloured O's correspond to the oxygen atoms of formate anions coordinating to copper ions. The red and magenta symbols correspond to the oxygen atoms that are located to the front and back of the copper hydroxide layer, respectively. (d) Molecular alignment of formate ions in **1**. Spheres correspond to O (red, magenta), C (dark grey), and H (light grey). Where the light grey formate ions are coordinating to the neighbouring copper hydroxide layer.

compound **1** exhibits a different magnetic behaviour to **2**, despite the structure of **1** resembling that of **2**.

Fig. 2(d) shows the molecular arrangements of the formate anions in the interlayers of **1**, in which the copper atoms and hydroxide ions are omitted, and the magenta spheres represent the oxygen atoms of the formate ions coordinated to the copper atoms. The grey formate ions are coordinated to the neighbouring copper hydroxide layer. Although interdigitated molecular arrangements are formed in **1** and **2**, the molecular interlayer packing of **1** is different to that of **2** (Fig. S3(d)†), as the formate ions in **1** are aligned toward the *b* axis to form a columnar structure. The molecular planes of the carboxylate groups in these columns are coplanar, in contrast to the tilted alignments of the formate ions in **2**. In addition, the formate ions in the interlayer of **1** are more densely packed than those in **2**. It should be noted that the molecular packing of the anion is related to the coordination positions of the copper ions in the inorganic layer and may significantly affect the magnetic interactions between copper ions.

## Magnetic properties

Fig. 3 outlines the magnetic properties of **1**, where the molar units of the paramagnetic susceptibility $\chi_p$ and magnetisation $M$ correspond to one mole of Cu(II). Fig. 3(a) shows the temperature dependence of the $\chi_p$ value of **1** during cooling at a rate of 10 K min$^{-1}$ at 500 Oe. The compound prepared herein exhibited magnetic behaviour similar to that of the sample prepared by Mori *et al.*[14] In addition, the $\chi_p$ value peaked at approximately 2.3 K, after which it decreased with further reductions in temperature; the maximum value of $\chi_p$ was 0.0420 emu mol$^{-1}$. Fig. 3(b) shows the temperature dependence of the product of $\chi_p$ and $T$ for this material, and it is noted that the $\chi_pT$ value decreased at lower temperatures. This observation suggests that antiferromagnetic interactions dominate in the copper hydroxide layer. The Curie and Weiss constants evaluated using the data recorded at $T > 100$ K were 0.521 emu K mol$^{-1}$ and −63.4 K, respectively. The magnetic data were then fitted to a two-dimensional regular triangular-lattice model, as follows:[23]

$$\chi_pT = C\left[1 + \sum_{n\geq 1}(\alpha_n/2^n n!)y^n\right] \quad (1)$$

where $T$ is temperature, $C$ is the Curie constant, $y$ is equal to $J/(k_BT)$, $J$ is the intermolecular exchange coupling constant and $k_B$ is the Boltzmann constant. This provides the average value of the magnetic interactions along the five different exchange paths. It is noted that antiferromagnetic exchange coupling constants are represented by positive values of $J$ ($J > 0$), while ferromagnetic ones are represented by negative values ($J < 0$). The coefficients $\alpha_n$ were determined to be: $\alpha_1 = 6$, $\alpha_2 = 48$, $\alpha_3 = 408$, $\alpha_4 = 3600$, $\alpha_5 = 42\,336$, $\alpha_6 = 781728$, $\alpha_7 = 13\,646\,016$, $\alpha_8 = 90\,893\,568$, and $\alpha_9 = -1798\,204\,416$. On the basis of eqn (1), the magnetic parameters for **1** were found to be: $C = 0.512$ emu K mol$^{-1}$ and $J/k_B = 35.7$ K by curve fitting above 50 K, as shown by the solid curve indicated in Fig. 3(b).

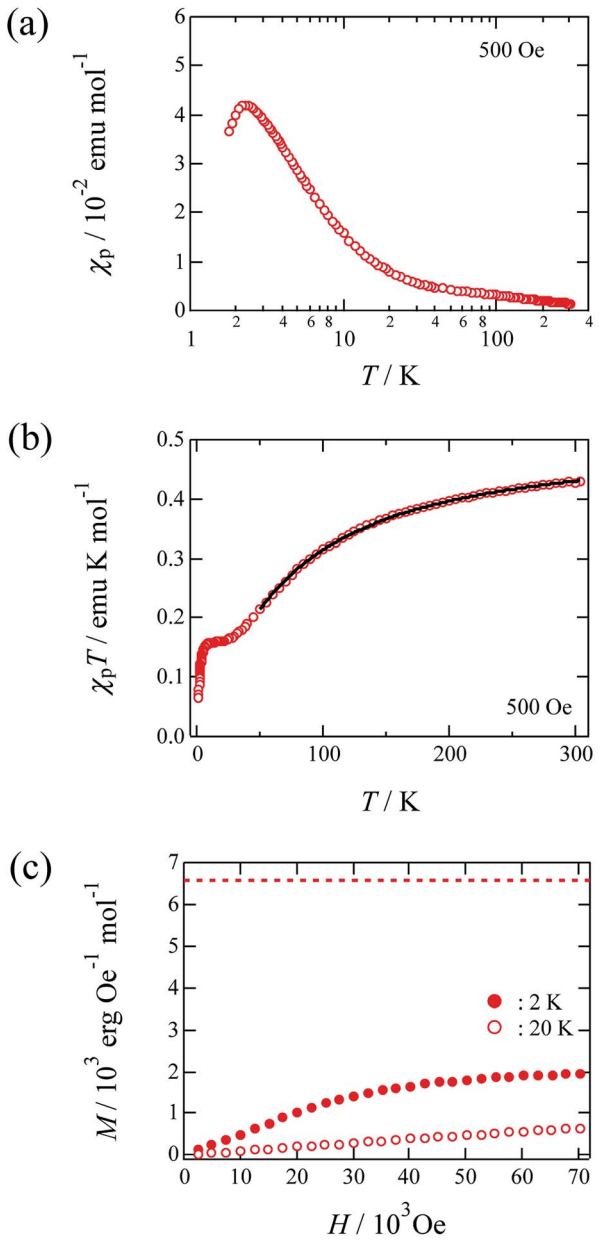


Fig. 3 Magnetic properties of **1**. The molar unit of $\chi_p$ and magnetization was chosen as the quantity per one mole of Cu. (a) Temperature dependence of the paramagnetic susceptibility $\chi_p$ for non-oriented microcrystals under 500 Oe. (b) The $\chi_pT$ *vs.* *T* plot for non-oriented microcrystals. The solid curves indicate the theoretical best fits of eqn (1). (c) Field dependence of the magnetization for non-oriented microcrystals of **1** at 2 K and 20 K.

Fig. 3(c) shows the field dependence of the magnetisation of **1** at 2 K. More specifically, the magnetisation value was observed to increase gradually with an increasing magnetic field, approaching a value of $2 \times 10^3$ erg $Oe^{-1}$ $mol^{-1}$ at approximately 70 kOe. This value is almost one-third of the theoretical value ($6.58 \times 10^3$ erg $Oe^{-1}$ $mol^{-1}$) of the saturation magnetisation with 1 mol where $S = 1/2$ and $g = 2.36$ spin,[17] as indicated by the broken line in Fig. 3(c). This magnetisation behaviour may corresponds to a 1/3-magnetisation plateau, which is commonly observed in two-dimensional triangular-lattice systems.[1] The magnetisation behaviour of this material at higher magnetic fields must therefore be investigated further.

Table 2 Magnetic parameters of **1**–**3**

| | **1** | **2** | **3** |
|---|---|---|---|
| $C$/emu K $mol^{-1}$ | 0.521 | 0.438 | 0.520 |
| $\theta$/K | −63.4 | +5.1 | +43.3 |
| $J/k_B$ | 35.7 | −0.7 | — |
| Intralayer magnetic interaction | Antiferromagnetic | Ferromagnetic | Ferromagnetic |
| $T_N$/K | 2.15 | 5.4 | 21.3 |
| Ground states | Antiferromagnet | Metamagnet | Metamagnet |
| Ref. | This work | 9 | 14 |

The magnetic parameters of the basic copper formates **1**–**3** are summarised in Table 2. In **1**, antiferromagnetic interactions dominantly work between the copper ions, while ferromagnetic interactions dominantly worked in **2** and **3**, and metamagnetic-like phase transitions were observed for **2** and **3** at 5.4 and 21.3 K, respectively, thereby revealing differences in the structures of the copper hydroxide layers and the intensities and signs of the intralayer magnetic interactions.

## Thermal properties

To investigate the magnetic anomaly at 2 K, the temperature dependence of the heat capacity $C_p$ of crystalline **1** was studied between 2 and 30 K, and the results are shown in Fig. 4. More specifically, the heat capacity exhibits a λ-shaped anomaly at 2.15 K, which supports the occurrence of a magnetic transition, likely due to antiferromagnetic ordering. The associated entropy change, $\Delta S$, was evaluated to be 1.94 J $K^{-1}$ $mol^{-1}$ by integration of the $C_p/T$ values over $T$; this value is smaller than the theoretical value for a magnetic ordering transition ($R$ ln 2 = 5.76 J $K^{-1}$ $mol^{-1}$),[24] which suggests that a short-range magnetic order,[17] a characteristic of low-dimensional magnets, occurs in the higher temperature region. This material has five magnetic-interaction pathways available to it; consequently, some of five magnetic interaction paths may have

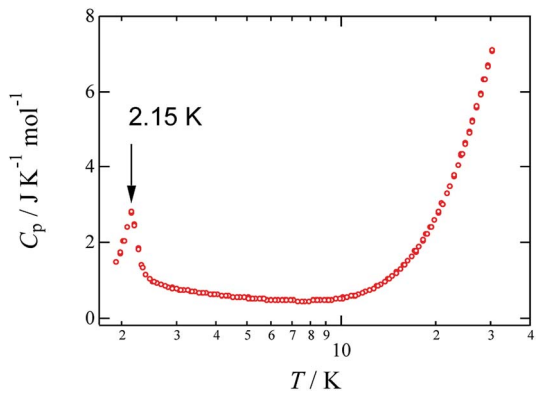


Fig. 4 Temperature dependence of heat capacity $C_p$ for **1**. The molar unit of $C_p$ was chosen as the quantity per one mole of Cu.

exchange coupling constants more than 50 K. Hereafter, it is necessary that the value of magnetic coupling constants of these magnetic interaction paths in this material are estimated.

## Conclusions

In this paper, crystal growth and magnetic studies of basic copper formate, $[Cu_3(OH)_4(HCOO)_2]$ (**1**) was herein reported. Three kinds of basic copper formate could be selectively and conveniently prepared as single crystals at appropriate concentrations and temperatures of copper formate solutions. The crystal structure of **1** was successively determined in this study. In terms of the magnetic properties, this material was found to have an $S = 1/2$ two-dimensional distorted triangular-lattice magnetic network with five kinds of magnetic interaction paths, where predominantly antiferromagnetic interactions exist between neighbouring copper ions at $J/k_B = 35.7$ K, in addition to antiferromagnetic ordering at 2.15 K. The magnetisation curve at 2 K corresponds to a 1/3-magnetisation plateau, which is commonly observed in two-dimensional triangular-lattice systems. The author believes that compound **1** is good candidate for a geometrical frustration system. The effect of geometrical frustration on the magnetic properties of this material will be examined in the future.

## Conflicts of interest

There are no conflicts to declare.

## Acknowledgements

This study was partially supported by the Daiko Foundation, by a Grant from the Faculty of Science and Technology, Seikei University, and by JSPS KAKENHI Grant Number 16K05942. X-ray structural analyses and magnetic measurements were conducted at the Institute of Molecular Science, supported by the Nanotechnology Platform Program (Molecule and Material Synthesis) of the Ministry of Education, Culture, Sports, Science and Technology (MEXT), Japan. Koichi Kikuchi is thanked for assistance with the elemental analyses.

## Notes and references

1 *Introduction to Frustrated Magnetism: Materials, Experiments, Theory*, ed. C. Lacroix, P. Mendels and F. Mila, Springer, 2011.
2 Y. Iitaka, S. Locchi and H. R. Oswald, *Helv. Chim. Acta*, 1961, **44**, 2095; M. P. Shores, E. A. Nytko, B. M. Bartlett and D. G. Nocera, *J. Am. Chem. Soc.*, 2005, **127**, 13462; G. Zheng, H. Kubozono, K. Nishiyama, W. Higemoto, T. Kawae, A. Koda and C. N. Xu, *Phys. Rev. Lett.*, 2005, **95**, 057201; H. Kikuchi, Y. Fujii, M. Chiba, S. Mitsudo, T. Idehara, T. Tonegawa, K. Okamoto, T. Sakai, T. Kuwai and H. Ohta, *Phys. Rev. Lett.*, 2005, **94**, 227201.
3 S.-H. Lee, H. Kikuchi, Y. Qiu, B. Lake, Q. Huang, K. Habicht and K. Kiefer, *Nat. Mater.*, 2007, **6**, 853; T.-H. Han, J. S. Helton, S. Chu, D. G. Nocera, J. A. Rodrigues- Rivera, C. Broholm and Y. S. Lee, *Nature*, 2012, **492**, 406.
4 M. A. Girtu, C. M. Wynn, W. Fujita, K. Awaga and A. J. Epstein, *Phys. Rev. B*, 1998, **57**, R11058; M. A. Girtu, C. M. Wynn, W. Fujita, K. Awaga and A. J. Epstein, *J. Appl. Phys.*, 1998, **293**, 7378; M. A. Girtu, C. M. Wynn, W. Fujita, K. Awaga and A. J. Epstein, *Phys. Rev. B*, 2000, **61**, 4117.
5 Y. Fujii, Y. Azuma, H. Kikuchi and Y. Yamamoto, *J. Phys.: Conf. Ser.*, 2009, **145**, 012061; S. Hara, H. Kondo and H. Sato, *J. Phys. Soc. Jpn.*, 2011, **80**, 043701.
6 W. Fujita and K. Awaga, *Inorg. Chem.*, 1996, **35**, 1915; W. Fujita, K. Awaga and T. Yokoyama, *Inorg. Chem.*, 1997, **36**, 196; W. Fujita and K. Awaga, *J. Am. Chem. Soc.*, 1997, **119**, 4563; W. Fujita, K. Awaga and T. Yokoyama, *Appl. Clay Sci.*, 1999, **15**, 281.
7 H. Effenberger, *Z. Kristallogr. Cryst. Mater.*, 1983, **165**, 127; S. Chu, P. Müller, D. G. Nocera and Y. S. Lee, *Appl. Phys. Lett.*, 2011, **98**, 092508.
8 A. Rujiwatra, C. J. Kepert and M. J. Rosseinsky, *Chem. Commun.*, 1999, 2307; A. Rujiwatra, C. J. Kepert, J. B. Claridge, M. J. Rosseinsky, H. Kumagai and M. Kurmoo, *J. Am. Chem. Soc.*, 2001, **123**, 10584; P. M. Forster, M. M. Tafoya and A. K. Cheetham, *J. Phys. Chem. Solids*, 2004, **65**, 11; F. Gándara, J. Perles, N. Snejko, M. Iglesias, B. Gómez-Lor, E. Gutiérres-Puebla and M. Á. Monge, *Angew. Chem., Int. Ed.*, 2006, **45**, 7998; D. T. Tran, N. A. Chernova, D. Chu, A. G. Oliver and S. R. J. Oliver, *Cryst. Growth Des.*, 2010, **10**, 974; H. Fei and S. R. J. Oliver, *Angew. Chem., Int. Ed.*, 2011, **50**, 9066.
9 H. Euler, B. Barbier, A. Kirfel, S. Haseloff, G. Eggert and Z. Kristallogr, *Z. Kristallogr.–New Cryst. Struct.*, 2009, **224**, 609; W. Fujita, K. Kikuchi and W. Mori, *Chem.–Asian J.*, 2012, **7**, 2830.
10 S. Švarcová, M. Klementová, P. Bezdička, W. Łasocha, M. Dušek and D. Hradil, *Cryst. Res. Technol.*, 2011, **46**, 1051.
11 W. Fujita and K. Kikuchi, *Bull. Chem. Soc. Jpn.*, 2013, **86**, 921.
12 S. Yoneyama, K. Kodama, K. Kikuchi, Y. Fujii, H. Kikuchi and W. Fujita, *CrystEngComm*, 2014, **16**, 1038; W. Fujita, *CrystEngComm*, 2015, **17**, 9193; W. Fujita, A. Tokumitu, Y. Fujii and H. Kikuchi, *CrystEngComm*, 2016, **18**, 8614.
13 Q. Evrard, C. Leuvrey, P. Farger, E. Delahaye, P. Rabu, G. Taupier, K. D. Dorkenoo, J.-M. Rueff, N. Barrier, O. Pérez and G. Rogez, *Cryst. Growth Des.*, 2018, **18**, 1809.
14 W. Mori and M. Kishita, *Inorg. Chim. Acta*, 1980, **42**, 11; H. Tamura, K. Ogawa, W. Mori and M. Kishita, *Inorg. Chim. Acta*, 1981, **54**, L87; K. Ueda, S. Takamizawa, W. Mori and K. Yamaguchi, *Mol. Cryst. Liq. Cryst.*, 1996, **286**, 17.
15 G. M. Sheldrick, *Acta Crystallogr.*, 2008, **A64**, 112.
16 G. M. Sheldrick, *SHELXL Version 2014/7*.
17 L. R. Carlin, *Magnetochemistry*, Springer-Verlag, Berlin, 1986.
18 M. J. Riban, *Bull. Soc. Chim. Fr.*, 1882, **38**, 113.
19 G. Fowles, *J. Chem. Soc., Dalton Trans.*, 1915, **107**, 1281.
20 A. F. Wells, *Structural Inorganic Chemistry*, Oxford University Press, London, 1975.
21 V. H. Crawford, H. W. Richardson, J. R. Wasson, D. J. Hodgson and W. E. Hattfield, *Inorg. Chem.*, 1976, **15**, 2107.

22 V. Molina, M. Rauhalahti, J. Hurtado, H. Fliegl, D. Sundholm and A. Muñoz-Castro, *Inorg. Chem. Front.*, 2017, **4**, 986; J. F. Torres, N. J. Bello-Vieda, M. A. Macías, A. Muñoz-Castro, C. Rojas-Dotti, J. Martínez-Lillo and J. Hurtado, *Eur. J. Inorg. Chem.*, 2018, 3644.

23 G. A. Baker Jr, H. E. Gilbert, J. Eve and G. S. Rushbrooke, *Phys. Rev.*, 1967, **164**, 800; G. A. Baker Jr, H. E. Gilbert, J. Eve and G. S. Rushbrooke, *Phys. Lett.*, 1967, **25A**, 207.

24 M. Sorai, M. Nakano and Y. Miyazaki, *Chem. Rev.*, 2006, **106**, 976.